Received: 8 Sep 2019 | Accepted: 8 Oct 2019 | Available online: 26 Dec 2019
DOI: http://dx.doi.org/10.18180/tecciencia.2019.27.10

TECCIENCIA

UNIVERSIDAD ECCI

RESEARCH ARTICLE

Engineering

Evaluation of Localization Strategies with the Meshless Method of Approximate Particular Solutions

Evaluación de estrategias de localización con el Método sin malla de Soluciones Particulares Aproximadas

Nelson F. Chaverra S. [1*] | **Maria C. Martínez L.** [1*] | **Juan D. Ríos G.** [1*] | **Julián M. Granados M** [1*]

[1]Institución Universitaria de Envigado

Correspondence
Nelson F. Chaverra S, Institución Universitaria de Envigado, Colombia
Email: nfchaverra@correo.iue.edu.co

The publication of this journal is funded by Universidad ECCI, Bogotá-Colombia.

Editors: Miguel Medina Jaime, Robert Paul Salazar

Editorial assistant : Luz Adriana Suáres Suáres.

How to cite
Nelson F. et al., **Evaluation of Localization Strategies with the Meshless Method of Approximate Particular Solutions**, TECCIENCIA, Vol. 14, No. 27, 103-113, 2019
DOI:http://dx.doi.org/10.18180/tecciencia.2019.27.10

ABSTRACT. In the present work, several localization schemes developed by the Method of Approximated Particular Solutions are evaluated. This meshless method uses solutions of a non-homogeneous Poisson auxiliary equation to approximate the dependent variable. Diffusion problems with Dirichlet and Neumann boundary conditions are selected to evaluate the performance of the localization strategy by using cross-shaped, cross- elongated shaped and circular neighborhoods. The results obtained with the cross-shaped neighborhoods show greater stability with respect to the shape parameter. Local formulations perform better on problems with Dirichlet boundary conditions while the global formulation obtains better results on diffusion problems with Neumann boundary conditions.

keywords: Particular solutions, Poisson equation, Analytic approximations.

RESUMEN. En el presente trabajo, se evalúan varios esquemas de localización con el Método de Soluciones Particulares Aproximadas (MAPS). Este método sin malla utiliza soluciones particulares de una ecuación auxiliar de Poisson no homogénea para aproximar la variable dependiente. Problemas de difusión con condiciones de frontera tipo Dirichlet y Neumann son abordados para evaluar el desempeño de la formulación local mediante el uso de vecindades en forma de cruz, cruz alargada y circular. Los resultados obtenidos con las vecindades en forma de cruz muestran una mayor estabilidad con respecto al parámetro de forma. Las estrategias de localización muestran un mejor desempeño en problemas con condiciones de frontera de Dirichlet, mientras que la formulación global obtiene mejores resultados en problemas de difusión con condiciones de frontera de Neumann.

Palabras clave: Soluciones particulares, Ecuación de Poisson, Aproximaciones analíticas.

[*] Equally contributing authors.

1 | INTRODUCTION

The Radial Basis Functions (RBF) are defined in terms of the Euclidean distance between two points, obtaining functions with radial symmetry if one of the points remains fixed. RFBs are easy to implement and It isn't affected by the problem dimension. Its potentiality has been studied since the 70's when Hardy [1] reported good results in its use as a two-dimensional scattered data interpolation strategy. In a study conducted by Franke [2] to evaluate the behavior of 29 interpolation algorithms, the author found that multi-quadric (MQ) RBF yielded the best results. A large number of methods that use RBF have been used in the solution of Partial Differential Equations (PDE) from the pioneering works of Kansa [3, 4] in which it was proposed to approximate the variable of the problem with a linear combination of RBF. Although this method showed great performance in solving flow problems, the system matrix tends to be ill-conditioned when a large number of nodes are used in the geometry. To overcome these difficulties is the indirect use of the RBF as proposed by Mai-Duy and Tran-Cong [5, 6] in such a way that the RBFs are used to approximate the derivatives of the problem variable instead of the variable itself as Kansa's method does. The results obtained in [5, 6] showed greater precision and better numerical stability in relation to the direct implementation of the RBF because the integration process has a smoother behavior than the derivation process.

Chen et al. [7] proposed the Method of Approximated Particular Solutions (MAPS) to solve linear Partial Differential Equations (PDE). In this method, an RBF is used as the source term of an auxiliary PDE in which the differential operator may be the same as the problem to be solved or part of it. The problem variable is approximated with a linear combination of particular solutions of the auxiliary PDE, obtained analytically. Although the vast majority of the global formulation of the MAPS has been implemented in the solution of scalar and linear problems [8, 9, 10, 11], it has recently been used to solve vector and nonlinear two-dimensional problems related to electrokinetic flows [12], Stokes flow [13], incompressible flow to high Reynolds numbers [14], electrically conductive flux in the presence of magnetic fields [14], among others, showing great potential for this meshless method. In all cases, a system of Stokes equations is taken as an auxiliary system and an MQ RBF is taken as the source term. The problems addressed in this work are solved with the MAPS proposed in [7] using as basis functions the particular solutions of the Poisson equation in which an MQ RBF is used as a source term.

Although global RBF-based methods tend to be very flexible and exhibit high-order convergence rates, systems with full matrices lead to the problem described by Shaback [15] as the uncertainty relation; better conditioning is associated with worse accuracy, and worse conditioning is associated with better accuracy. As the system size increases, this problem becomes more pronounced. Many techniques have been developed to reduce the effect of the uncertainty relationship, such as RBF-specific pre-conditioners and adaptive data center selection. However, at present the only reliable method to control numerical ill-conditioning and computational cost as the size of the problem increases is domain decomposition or localization strategies. One of the first attempts in this direction was made by Lee et al. [16] who proposed the local MQ approach in which only the nodes within the influence subdomain of a central node are used in the asymmetric method to solve the Poisson equation. This work was followed by others who have explored various strategies for RBF-based methods [17, 18, 19]. The development of localization schemes for the MAPS has become a topic of interest in recent years. Among others, it is worth mentioning the proposals made in the references [20, 21, 22] in which neighborhoods with five nodes in two-dimensional problems and neighborhoods with seven nodes for three-dimensional problems are considered. In this work, a localization strategy for the MAPS is implemented through the use of cross-shaped, elongated and circular cross neighborhoods. The elongated cross-shaped neighborhood is considered by the authors as an alternative to the cross-shaped and circular-shaped neighborhoods widely studied in the literature. The goal of this work is to solve diffusion problems in a two-dimensional cavity to evaluate the behavior of the global formulation of the MAPS compared to the local formulation considering different shapes and sizes of neighborhoods. Additionally, the results obtained with both formulations are compared with the results reported in [20] when solving a Poisson equation through the use of the global formulation of the MAPS and a localization strategy similar to one of those implemented in this work. This article is structured as follows: the section 2 presents the problem to be solved. The global and local formula-

tions for the MAPS are described in section 3. Numerical examples showing the results obtained with all the schemes are addressed in section 4.

2 | GOVERNING EQUATION

Let be Ω a two-dimensional region with boundary Γ, and u a scalar function satisfying a Laplace equation. This boundary value problem (BVP) is defined as follows

$$\begin{aligned} \Delta \boldsymbol{u}(\boldsymbol{x}) &= 0, \qquad \boldsymbol{x} \in \Omega, \\ \boldsymbol{B}\boldsymbol{u}(\boldsymbol{x}) &= \boldsymbol{g}(\boldsymbol{x}), \quad \boldsymbol{x} \in \Gamma \end{aligned} \tag{1}$$

where g is a known function, B is a Dirichlet or Neumann boundary operator and $\boldsymbol{x}$ is a point in $\Omega \cup \Gamma$. Additionally, Γ_D y Γ_N are set of boundary nodes where Dirichlet and Neumann conditions are imposed, respectively. We consider regular nodal distributions with N_B nodes in the boundary, N_{BD} boundary nodes with Dirichlet condition, N_{BN} boundary nodes with Neumann conditions and N_I nodes in Ω where $N_B + N_I = N_{BD} + N_{BN} + N_I = N$.

3 | LOCALIZATION METHOD

The Method of Approximate Particular Solutions (MAPS) is part of the meshless methods based on Radial Basis Functions (RBF) and is used in this work to solve the (BVP) (1) in the plane. The MAPS is indirect because it does not use the BVP as base functions in the proposed interpolation to approximate the variable values in the problem. This section presents the global (GMAPS) and local (LMAPS) formulation of the method. First, the fundamentals of the GMAPS are reviewed as proposed in [7], then the local formulation implemented for the MAPS is studied in this work.

3.1 | Global formulation

The GMAPS proposes approximate the BVP solution with a function $\hat{\boldsymbol{u}}$ found with a superposition of basis functions as follows

$$\tilde{\boldsymbol{u}}(\boldsymbol{x}) = \sum_{j=1}^{N} \alpha_j \psi(\boldsymbol{r}_j), \tag{2}$$

where $\{\alpha_j\}_{j=1}^{N}$ is a set of real coefficients and ψ is the particular solution of the the following auxiliary equation

$$\nabla^2 \psi(\boldsymbol{r}) = \phi(\boldsymbol{r}). \tag{3}$$

In this document a multi-quadratic (MQ) RBF is used as source term in Eq. (3) since other authors reported relevant improvements of this function choice by comparing it with other RBF. In particular, a exponential error convergence and positive localization matrices are reported in [23][24] when the interpolation scheme is used. Hence, $\phi(r) = \sqrt{r^2 + c^2}$ and

$$\psi(\boldsymbol{r}) = \frac{1}{9}(4c^2 + r^2)\sqrt{c^2 + r^2} - \frac{c^3}{3}\ln\left(c + \sqrt{c^2 + r^2}\right), \tag{4}$$

where c is the shape parameter and $r = r(\boldsymbol{x}) = |\boldsymbol{x} - \boldsymbol{\xi}|$ is the Euclidean distance between a trial node at $\boldsymbol{x}$ and the source node $\boldsymbol{\xi}$. In the current document both nodes are included in the local distribution in each case, thus the following notation is used

$$\boldsymbol{r}_j(\boldsymbol{r}) = |\boldsymbol{x} - \boldsymbol{\xi}_j| \quad \text{and} \quad \psi_i(\boldsymbol{r}_j) = \psi(\boldsymbol{r}_j(\boldsymbol{x}_i)) = \psi(|\boldsymbol{x}_i - \boldsymbol{\xi}_j|). \tag{5}$$

The approximation given by Eq. (2) is forced to fulfill the partial differential equation PDE as well as the boundary conditions, then the following relationships

$$\nabla^2 \tilde{u}(x) = \sum_{j=1}^{N} \alpha_j \nabla^2 \psi(\boldsymbol{r}_j) = \sum_{j=1}^{N} \alpha_j \phi(\boldsymbol{r}_j) = 0 \quad \text{and} \quad \boldsymbol{B}\tilde{\boldsymbol{u}}(\boldsymbol{x}) = \sum_{j=1}^{N} \alpha_j \boldsymbol{B}\psi(\boldsymbol{r}_j) = \boldsymbol{g}(\boldsymbol{x}) \tag{6}$$

must be satisfied. The first one is a consequence of Eq. (3). Eqs. (3) to (6) show that the GMAPS is an indirect method since the FRB is used as source term in the auxiliary Eq. (3) rather than base function in Eq. (2). On the other hand, the MQ RBF is used to approximate derivatives of the variable, thus a integration is required to obtain a close form of ψ. This goal is achieved by using a procedure to remove singularities in the function by eliminating terms responsible of the singularity. If the Eq. (6) is satisfied in the inner and boundary nodes respectively and assuming a numbering where boundary nodes are first, then it is found

$$\begin{bmatrix} \boldsymbol{B}\psi_1(\boldsymbol{r}_1) & \cdots & \boldsymbol{B}\psi_1(\boldsymbol{r}_N) \\ \vdots & & \vdots \\ \boldsymbol{B}\psi_{N_B}(\boldsymbol{r}_1) & \cdots & \boldsymbol{B}\psi_{N_B}(\boldsymbol{r}_N) \\ \phi_{N_B+1}(\boldsymbol{r}_1) & \cdots & \phi_{N_B+1}(\boldsymbol{r}_N) \\ \vdots & & \vdots \\ \phi_N(\boldsymbol{r}_1) & \cdots & \phi_N(\boldsymbol{r}_N) \end{bmatrix} \begin{bmatrix} \alpha_1 \\ \vdots \\ \alpha_{N_B} \\ \alpha_{N_B+1} \\ \vdots \\ \alpha_N \end{bmatrix} = \begin{bmatrix} \boldsymbol{g}(\boldsymbol{x}_1) \\ \vdots \\ \boldsymbol{g}(\boldsymbol{x}_{N_B}) \\ 0 \\ \vdots \\ 0 \end{bmatrix}. \tag{7}$$

The values found for the set $\{\alpha_j\}_{j=1}^{N}$ by solving the system defined in Eq. (7) are replaced in the linear combination given by Eq. (2) to calculate $\tilde{\boldsymbol{u}}$. The matrix in Eq. (7) tends to be ill-conditioned as the number of nodes in $\Omega \cup \Gamma$ grows. Some authors have implemented strategies to face this problem with the aim to avoid inaccuracies it their results.

3.2 | Local Formulation

In order to reduce the computation time, due to the construction of a dispersed matrix associated to the system of equations, in this work a local formulation of the MAPS is used in which several types of neighborhoods for the nodes in the geometry are considered: neighborhood is cross-shaped, neighborhood in the form of elongated cross and circular neighborhood. The procedure described below is implemented for each neighborhood.

Let us define $\{\boldsymbol{x}_i\}_{i=1}^{N}$ as a nodal distribution in $\Omega \cup \Gamma$. For each $\boldsymbol{x}_i \in \Omega \cup \Gamma_N$ a neighbourhood is built, $V(\boldsymbol{x})$, where $\boldsymbol{x}$ is included and several close nodes are chosen according to the neighborhood shape. Hence, if $\boldsymbol{x} \in \Omega \cup \Gamma_N$ then $V(\boldsymbol{x}) = \{\boldsymbol{x}_{i(k)}\}_{k=1}^{n_i}$, where n_i is the number of nodes in the neighborhood and $\boldsymbol{x}_{i(k)}$ is a local indexation. The set of neighborhoods satisfies $V(\boldsymbol{x}_i) \cap V(\boldsymbol{x}_j) \neq 0$ for some values of i and j. The interpolation in Eq. (2) is used at each neighborhood to approximate u through a set of $N_{BN} + N_I$ functions $\tilde{u}$. The following interpolation

$$\tilde{\boldsymbol{u}}(\boldsymbol{x}) = \sum_{k=1}^{n_i} \alpha_{i(k)} \psi(\boldsymbol{r}_{i(k)}) \tag{8}$$

is proposed for each $\boldsymbol{x} \in V(\boldsymbol{x}_i)$. In this case, the sub-index $i(k)$ refers to a local indexing where $r_{i(k)} = r_{i(k)}(\boldsymbol{x}) = |\boldsymbol{x} - \boldsymbol{x}_{i(k)}|$. The localization of the interpolation given by Eq. (8) in each node of $V(\boldsymbol{x}_i)$ results in a relationship among interpolation coefficients and the values of $\tilde{u}$ in the ith-neighbourhood with the following matrix system

$$\begin{bmatrix} \tilde{\boldsymbol{u}}(\boldsymbol{x}_{i(1)}) \\ \tilde{\boldsymbol{u}}(\boldsymbol{x}_{i(2)}) \\ \vdots \\ \tilde{\boldsymbol{u}}(\boldsymbol{x}_{i(n_i)}) \end{bmatrix} = \begin{bmatrix} \psi_{i(1)}(\boldsymbol{r}_{i(1)}) & \psi_{i(1)}(\boldsymbol{r}_{i(2)}) & \cdots & \psi_{i(1)}(\boldsymbol{r}_{i(n_i)}) \\ \psi_{i(2)}(\boldsymbol{r}_{i(1)}) & \psi_{i(2)}(\boldsymbol{r}_{i(2)}) & \cdots & \psi_{i(2)}(\boldsymbol{r}_{i(n_i)}) \\ \vdots & \vdots & & \vdots \\ \psi_{i(n_i)}(\boldsymbol{r}_{i(1)}) & \psi_{i(n_i)}(\boldsymbol{r}_{i(2)}) & \cdots & \psi_{i(n_i)}(\boldsymbol{r}_{i(n_i)}) \end{bmatrix} \begin{bmatrix} \alpha_{i(1)} \\ \alpha_{i(2)} \\ \vdots \\ \alpha_{i(n_i)} \end{bmatrix} \tag{9}$$

where $\psi_{i(j)}(r_{i(k)})$ is understood according to the notation defined in Eq. (5). The right hand side matrix in Eq. (9) is not singular (see Duchon [25]) and it is denoted as Ψ_i, therefore

$$\begin{bmatrix} \alpha_{i(1)} \\ \alpha_{i(2)} \\ \vdots \\ \alpha_{i(n_i)} \end{bmatrix} = [\Psi_i]^{-1} \begin{bmatrix} \tilde{\boldsymbol{u}}(\boldsymbol{x}_{i(1)}) \\ a\tilde{\boldsymbol{u}}(\boldsymbol{x}_{i(2)}) \\ \vdots \\ \tilde{\boldsymbol{u}}(\boldsymbol{x}_{i(n_i)}) \end{bmatrix}. \tag{10}$$

The interpolation (8) is used to build the system of algebraic equations associated to the problem by imposing the differential operator or the one defined in the boundary when $V(\boldsymbol{x}_i)$ corresponds to an inner point $\boldsymbol{x}_i \in \Omega$ or a boundary point $\boldsymbol{x}_i \in \Gamma_N$ respectively. Eq. (10) allows to establish a straightforward procedure in the LMAPS where the unknowns of the algebraic system of equations are values of $\tilde{u}$ for each $\boldsymbol{x} \in \Omega \cup \Gamma_N$, $\{\tilde{u}_k\}_{k=1}^{N_{BN}+N_I}$, instead of the set of coefficients as occurs in the GMAPS.

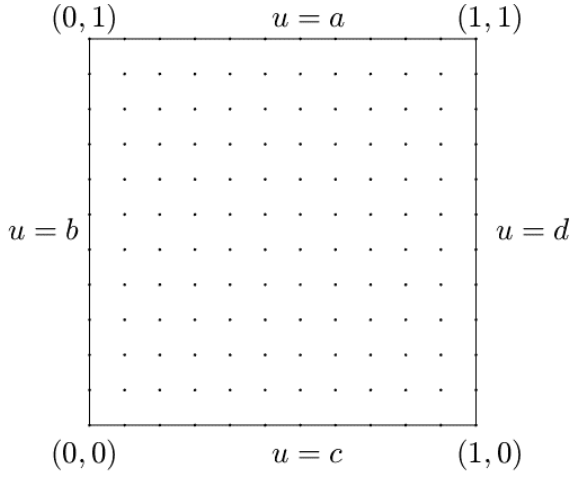

(a) Geometry used the study in all cases with uniform distribution.

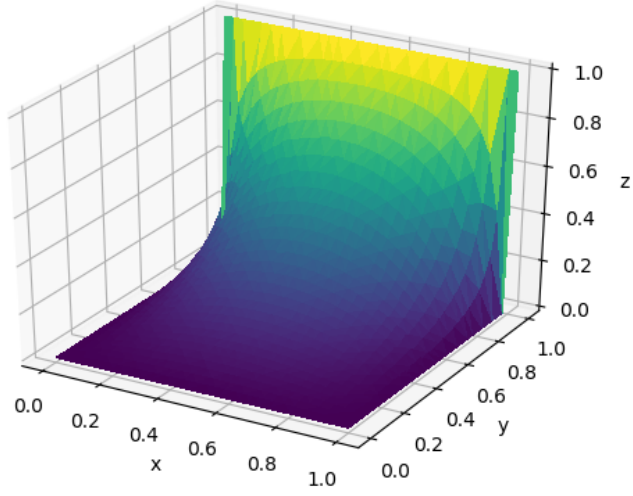

(b) Analytical solution of the case 1 in section 4.1.

FIG. 1 Domain and analytical solution.

The interpolation in Eq. (8) is forced to fulfill the differential equation and the boundary conditions taking

into account Eqs. (3) and (10), as a result

$$\nabla^2\tilde{\boldsymbol{u}}(\boldsymbol{x}_i) = \sum_{k=1}^{n_i}\alpha_k\nabla^2\psi(\boldsymbol{r}_{i(k)}) = \left[\phi_i(\boldsymbol{r}_{i(1)}),\phi_i(\boldsymbol{r}_{i(2)}),\ldots,\phi_i(\boldsymbol{r}_{i(n_i)})\right][\Psi_i]^{-1}\begin{bmatrix}\tilde{\boldsymbol{u}}(\boldsymbol{x}_{i(1)})\\ \tilde{\boldsymbol{u}}(\boldsymbol{x}_{i(2)})\\ \vdots\\ \tilde{\boldsymbol{u}}(\boldsymbol{x}_{i(n_i)})\end{bmatrix}, \qquad \boldsymbol{x}_i \in \Omega \tag{11}$$

$$\boldsymbol{B}\tilde{\boldsymbol{u}}(\boldsymbol{x}_i) = \sum_{k=1}^{n_i}\alpha_k\boldsymbol{B}\psi(\boldsymbol{r}_{i(k)}) = \left[\boldsymbol{B}\psi_i(\boldsymbol{r}_{i(1)}),\boldsymbol{B}\psi_i(\boldsymbol{r}_{i(2)}),\ldots,\boldsymbol{B}\psi_i(\boldsymbol{r}_{i(n_i)})\right][\Psi_i]^{-1}\begin{bmatrix}\tilde{\boldsymbol{u}}(\boldsymbol{x}_{i(1)})\\ \tilde{\boldsymbol{u}}(\boldsymbol{x}_{i(2)})\\ \vdots\\ \tilde{\boldsymbol{u}}(\boldsymbol{x}_{i(n_i)})\end{bmatrix}, \qquad \boldsymbol{x}_i \in \Gamma_N$$

A system of equations associated to a dispersed matrix is obtained from Eq. (11) and its solution allows to find $\{\tilde{u}_k\}_{k=1}^{N_{BN}+N_I}$.

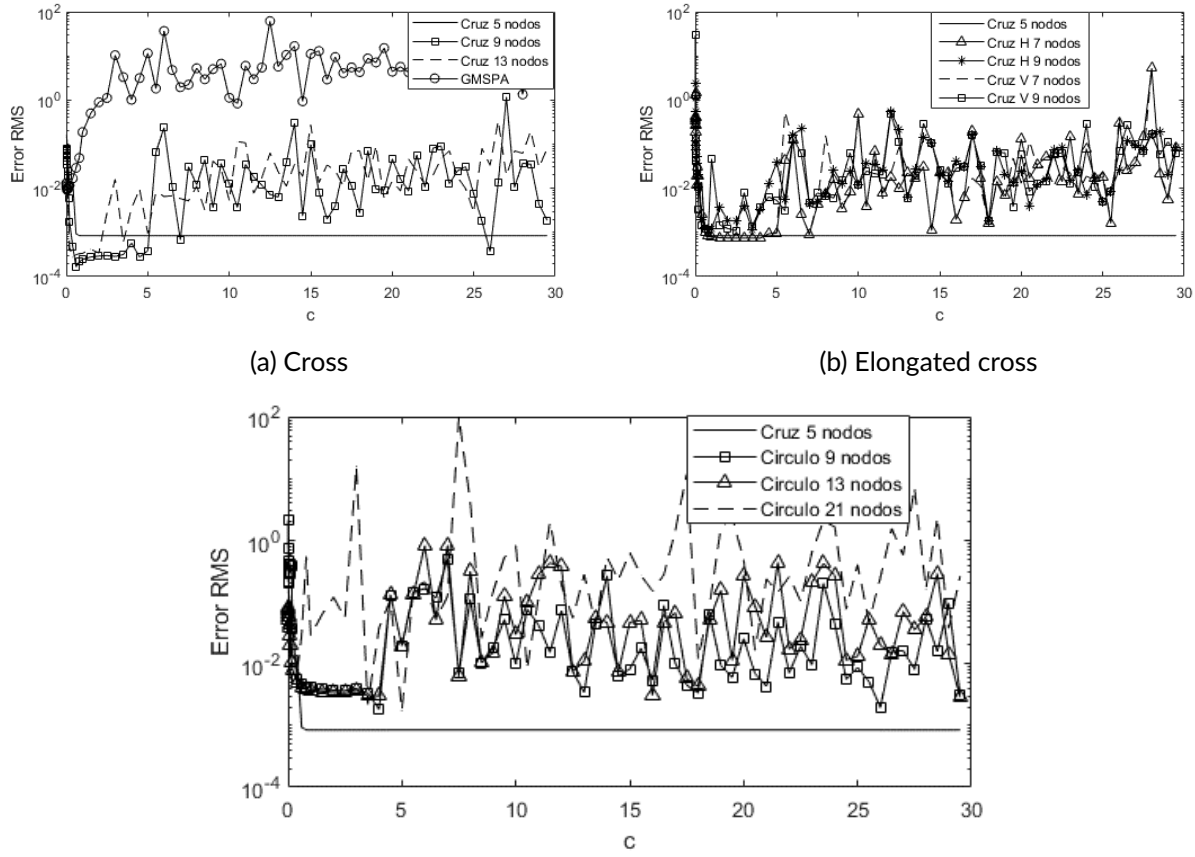

(a) Cross

(b) Elongated cross

(c) Circular

FIG. 2 RMS Error vs the shape parameter for different neighborhoods under Dirichlet boundary conditions.

4 | RESULTS

The global and local formulation of the MAPS shown in Section 3 are used to solve Eq. (2) under Dirchlet and Neumann boundary conditions. Results are obtained using uniform nodal distributions of $5 \times 5, 10 \times 10, 17 \times 17$ and 31×31 nodes on the region $[0, 1] \times [0, 1]$. Fig. 1 - (a) shows the geometry and one of the nodal distribution. The cases considered have analytic solution which allows to compute the error as follows

$$Error_{RMS} = \sqrt{\frac{1}{n} \sum_{k=1}^{N} |\boldsymbol{u}_i - \tilde{\boldsymbol{u}}_i|^2} \tag{12}$$

where u and $\tilde{u}$ are the analytical and numerical solution respectively.

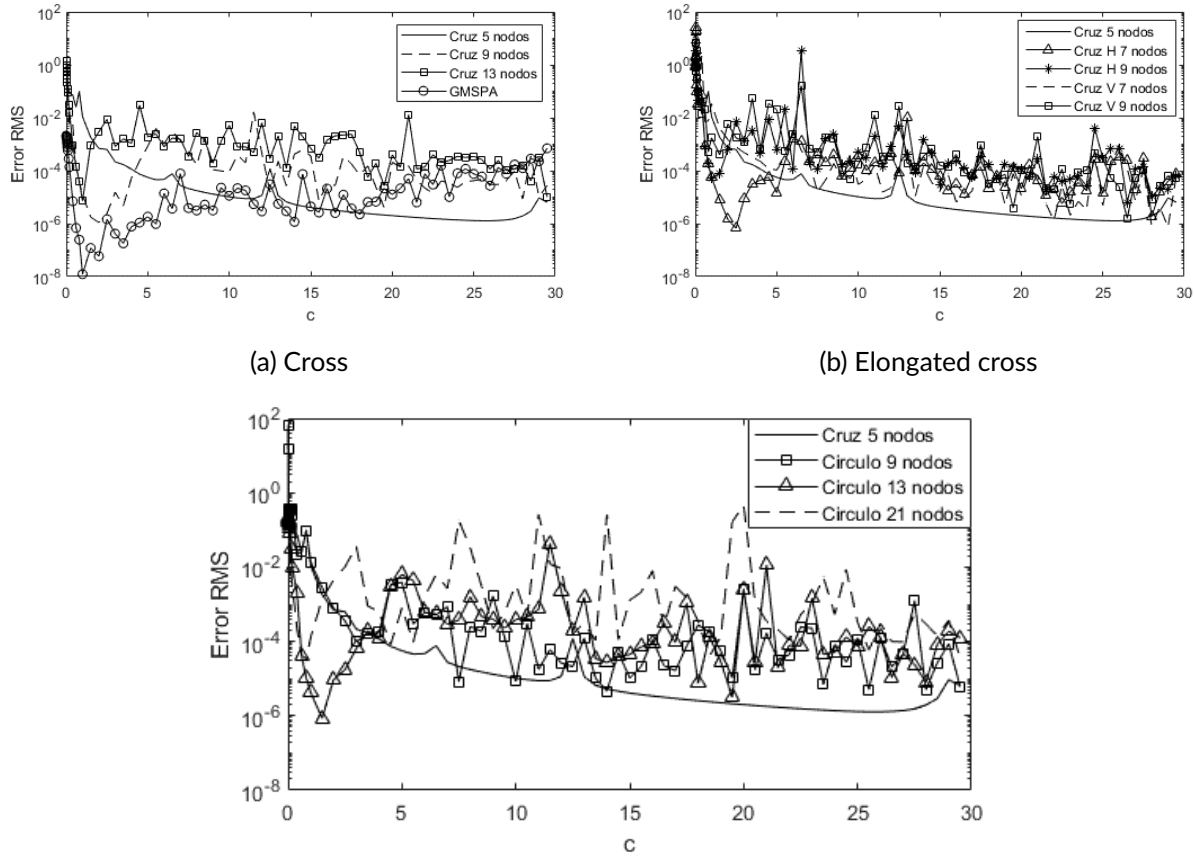

(a) Cross

(b) Elongated cross

(c) Circular

FIG. 3 RMS Error vs the shape parameter for different neighborhoods under Neumann boundary conditions.

4.1 | Study cases with Dirchlet boundary conditions

Four neighborhoods are used in the current study to implement the local scheme: cross, cross H (horizontally elongated), cross V (vertically elongated), and the circle. In this work, we propose to compare elongated cross neighborhoods with cross and circular neighborhoods commonly studied by other authors. Additionally, four configurations with Dirchlet boundary conditions are considered on the geometry sides in Fig. 1 to validate

the global and local MAPS (see Table 1).

TABLE 1 Study cases for the GMAPS and LMAPS with Dirchlet boundary conditions

	case 1	case 2	case 3	case 4
a	1	1	1	1
b	0	1	0	1
c	0	0	1	1
d	0	0	0	0

The case 1 and the distribution of 17×17 nodes ares used to find the optimal value of c for the global and local MAPS. Fig. 1 - (b) shows the analytical solution for the case 1. Fig. 2 shows the behaviour of the error as a function of c. The error profile of the GMAPS is larger than the one computed in the LMAPS at any neighborhood since the localization strategies reproduce better the gradients of u in Ω. All types of neighborhoods (except the cross of 5 nodes) change importantly with c and its associated error tends to grow as c is increased. Similarly, error in the LMAPS decreases for small values of c. Such error becomes smaller as the number of nodes in the neighborhood is increased. This behaviour occurs since the profiles of the LMAPS approach to the GMSPA profiles as the number of nodes becomes larger. Error in the circular neighborhood is even larger than error in the enlarged cross studied in this document. Neighborhood corresponding to a cross with 9 nodes behaves well for small values of $c \in [0.4, 5]$ where error does not change importantly with this parameter even when its behaviour can change drastically for larger values of c.

TABLE 2 Optimal values in the global and local MAPS for each neighborhood type in the case 1.

	Global	Cross			Cross H		Cross V		Circular		
Nodes	289	5	9	13	7	9	7	9	9	13	21
c	0.05	3.5	0.6	0.4	3.5	0.8	3.5	2.5	4	29.5	5
RMS$^{(a)}$ error	92.37	8.42	1.66	2.69	7.41	11.26	7.36	10.98	18.34	28.88	17.38

$^{(a)}$ All the RMS error values are multiplied by 10^{-4}

The optimal values of c in the interval $(0, 30]$ and its root-mean-square (RMS) error associated to each neighborhood are shown in Table 2. The error in the global strategy is larger than the one computed for the optimal values of c in other cases. It implies that the local MAPS reproduce better the gradients in Ω when Dirichlet boundary conditions are considered. RMS error found in the elongated cross and cross neighborhoods are similar. The RMS error profiles of the elongated cross and circular neighborhoods with 9 and 13 nodes show a similar growing behaviour. However, better results are obtained when optimal values of c are used in the elongated cross case as it is shown in Fig. 2 and Table 2.

4.2 | Study cases with Neumann boundary conditions

In this section the MAPS formulation is presented by using the solution of problem given by Eq. (2) on the unit square shown in Fig. 1. The Dirchlet and Neuman Boundary conditions of the problem are defined by

$$\begin{aligned} u(x_1, 0) &= 0, & x_1 \in [0,1] \\ u(x_1, 1) &= 1, & x_1 \in [0,1] \\ \frac{\partial u}{\partial x_1}(0, x_2) = \frac{\partial u}{\partial x_1}(1, x_2) &= 0, & x_2 \in [0,1] \end{aligned} \tag{13}$$

The gradients of the analytical solution are constant then the expected error is small. The error profiles RMS with respect the shape parameter on the 17×17 nodal uniform distribution is shown in Fig. 3. Those profiles change with c as occurs with the Dirichlet boundary problem. An exception is the cross with 5 nodes. The RMS error decreases as c grows in the local MAPS formulation which uses the cross with 5 nodes. Errors asso-

ciated to elongated cross-shaped neighborhoods behave similar to the ones computed for the cross-shaped neighborhoods. The RMS error profile of the globla MAPS is optimal when c is small. The best behavior of the GMSPA error profile in this case is related to the type of problem in which a constant gradient is considered. Additionally, the results suggest that global MAPS reproduce better the Neumman boundary conditions than local MAPS.

TABLE 3 RMS error for both formulations considering the 4 cases described in Table 2.

	Formulation	5×5	10×10	17×17	31×31
Case 1	Gobal MAPS$^{(a)}$	0.032464935	0.016508911	0.009237024	0.005080164
	Cross with 5 nodes$^{(b)}$	0.003489350	0.001605290	0.000842775	0.000461830
Case 2	Gobal MAPS	0.022073199	0.01223995	0.007258954	0.004264315
	Cross with 5 nodes	0.003896699	0.001539830	0.000836309	0.000455119
Case 3	Gobal MAPS	0.0548441	0.026071524	0.014397534	0.007817114
	Cross with 5 nodes	0.004424285	0.002166386	0.001196665	0.000650008
Case 4	Gobal MAPS	0.029364895	0.014530504	0.008384832	0.00478309
	Cross with 5 nodes	0.003605916	0.000532882	0.000075190	0.000008358

$^{(a)}$ where $c = 0.05$

$^{(b)}$ where $c = 3.5$

Optimal values of $c \in (0, 30]$ for both formulations including four types of neighborhoods are shown in Table 4. The smaller RMS error for the optimal value of c corresponds to the global MAPS since the analytical solution reproduce better the constant gradient. The RMS error profile of the global MAPS tends to grow but it is damped. Similarly, the local MAPS may not reproduce properly the Neumann boundary conditions. A similar profile behaviour is observed in the elongated cross and circular neighborhoods having 9 and 13 nodes, where profiles preserve near the error profile of the cross neighborhood with 5 nodes.

5 | CONCLUSIONS

In this work the global and local MAPS are implemented. Both formulations are used to solve diffusion problems in the unitary cavity under Dirchlet and Neumann Boundary Conditions. Four neighborhoods are defined in the local formulation : cross, horizontal elongated cross, vertical elongated cross and Circular. A error sensibility study is performed of each case in terms of the shape parameter c.

The results show that global and local formulations depends drastically on c, then it is necessary to find an optimal value of this parameter. Optimal values of c in the global MAPS are small. On the other hand, optimal values of the shape parameter are large in the local formulation. This optimal value decreases as the node number grows, which shows that local scheme approaches to global one when a large value of nodes are employed. Results obtained in the current study (Laplace problem) and the ones reported in [20] (Poisson problem) show that the RMS error dependence with c are similar. Both studies show that increasing the number of nodes in the neighborhood under Neumann boundary conditions can affect the local MAPS performance.

References

[1] R. Hardy, "Multiquadric equations of topography and other irregular surfaces," *J. Geophys. Res*, vol. 76, p. 1905–1915, 1971. doi: 10.1029/JB076i008p01905

[2] R. Franke, "Scattered data interpolation: Test of some methods," *Math. Comput*, vol. 38, p. 181–199, 1982. https://www.jstor.org/stable/2007474?seq=1.

[3] E. Kansa, "Multiquadrics – a scattered data approximation scheme with applications to computational fluid-dynamics i," *Comput. Math. Appl*, vol. 19, p. 127–145, 1990. doi: 10.1016/0898-1221(90)90270-T

[4] E. Kansa, "Multiquadrics – a scattered data approximation scheme with applications to computational fluid-dynamics ii," *Comput. Math. Appl*, vol. 19, p. 147–161, 1990. doi: 10.1016/0898-1221(90)90271-K

[5] N. Mai-Duy and T. Tran-Cong, "Numerical solution of differential equations using multiquadric radial basis function networks," *Neural Netw*, vol. 14, p. 185–199, 2001. doi: 10.1016/S0893-6080(00)00095-2

[6] N. Mai-Duy and T. Tran-Cong, "Approximation of function and its derivatives using radial basis function networks," *Appl. Math. Model*, vol. 27, p. 197–220, 2003. doi: 10.1016/S0307-904X(02)00101-4

[7] C. Chen, C. Fan, and P. Wen, "The method of approximate particular solutions for solving certain partial differential equations," *Numer. Methods Partial Diff. Equ*, vol. 28, p. 506–522, 2012. doi: 10.1002/num.20631

[8] C. Chen, C. Fan, and P. Wen, "The method of approximate particular solutions for solving elliptic problems with variable coefficients," *Int. J. Comput. Methods*, vol. 8, p. 545–559, 2011. doi: 10.1142/S0219876211002484

[9] P. Wen and C. Chen, "The method of particular solutions for solving scalar wave equations," *Int. J. Numer. Meth. Bio*, vol. 26, p. 1878–1889, 2010. doi: 10.1002/cnm.1278

[10] S. Reutskiy, "Method of particular solutions for nonlinear poisson-type equations in irregular domains," *Eng. Anal. Bound. Elem*, vol. 37, p. 401–408, 2013. doi: 10.1016/j.enganabound.2012.11.010

[11] Z. Fu, W. Chen, and L. Ling, "Method of approximate particular solutions for constant- and variable-order fractional diffusion models," *Eng. Anal. Bound. Elem*, vol. 57, p. 37–46, 2015. doi: 10.1016/j.enganabound.2014.09.003

[12] D. A. C. et Al., "Método de Soluciones Particulares Aproximadas Para la Solución de Fluidos Electro-Cinéticos en Micro y Nanocanales," *TECCIENCIA*, vol. 14, p. 85–101, 2019. doi: 10.18180/tecciencia.2019.27.9

[13] J. Granados, H. Power, C. Bustamante, W. Flórez, and A. Hill, "A global particular solution meshless approach for the four-sided lid-driven cavity flow problem in the presence of magnetic fields," *Computers & Fluids*, vol. 160, pp. 120–137, 2018. doi: 10.1016/j.compfluid.2017.10.027

[14] J. G. Morales, H. Power, C. Bustamante, and W. Flórez, "Influence of magnetic fields on simultaneous stationary solutions of two-dimensional sudden expansion channel flow at low re m," *Fluid Dynamics Research*, vol. 50, no. 5, p. 051416, 2018. doi: 10.1088/1873-7005/aace32

[15] R. Schaback, "Multivariate interpolation and approximation by translates of a basis function," *Approximation Theory*, vol. VIII, Vol. 1, p. 491–514, 1995.

[16] C. Lee, X. Liu, and S. Fan, "Local multiquadric approximation for solving boundary value problems," *Comput. Mech*, vol. 30, p. 396–409, 2003. doi: 10.1007/s00466-003-0416-5

[17] E. Divo and K. Kassab, "An efficient localised radial basis function collocation method for fluid flow and conjugate heat transfer," *J. Heat Transfer*, vol. 212, p. 99–123, 2006. doi: 10.1115/1.2402181

[18] B. Sarler and R. Vertnik, "Meshless explicit local radial basis function collocation methods for diffusion problems," *Comput. Math. Appl*, vol. 51, p. 1269–1282, 2006. doi: 10.1016/j.camwa.2006.04.013

[19] D. Stevens, H. Power, M. Lees, and H. Morvan, "The use of pde centres in the local rbf hermitian method for 3d convective-diffusion problems," *J. Comput. Phys*, vol. 228, p. 4606–4624, 2009. doi: 10.1016/j.jcp.2009.03.025

[20] G. Yao, J. Kolibal, and C. Chen, "A localized approach for the method of approximate particular solutions," *Comput. Math. Appl*, vol. 61, p. 2376–2387, 2011. doi: 10.1016/j.camwa.2011.02.007

[21] G. Yao, S. Islam, and B. Šarler, "Assessment of global and local meshless methods based on collocation with radial basis functions for parabolic partial differential equations in three dimensions," *Eng. Anal. Bound. Elem*, vol. 36, p. 1640–1648, 2012. doi: 10.1016/j.enganabound.2012.04.012

[22] C. Lin, M. Gu, D. Young, J. Sladek, and V. Sladek, "The localized method of approximated particular solutions for solving two-dimensional incompressible viscous flow field," *Eng. Anal. Bound. Elem*, vol. 57, p. 23–36, 2015. doi: 10.1016/j.enganabound.2014.11.035

[23] W. Madych, "Miscellaneous error bounds for multiquadric and related interpolators," *Comput. Math. Appl*, vol. 24, p. 121–138, 1992. doi: 10.1016/0898-1221(92)90175-H

[24] C. Micchelli, "Interpolation of scattered data: Distance matrices and conditionally positive definite functions," *Constr. Approx*, vol. 2, p. 11–22, 1986. doi: 10.1007/BF01893414

[25] J. Duchon, "Splines minimizing rotation invariant semi-norms in sobolev spaces: constructive theory of functions of several variables," *Lecture Notes in Mathematics. Springer-Verlag*, vol. 571, p. 85–110, 1976. doi: 10.1007/BFb0086566